# Vacuum Rabi splitting in semiconductors

The recent development of techniques to produce optical semiconductor cavities of very high quality has prepared the stage for observing cavity quantum-electrodynamic effects in solid-state materials. Among the most promising systems for these studies are semiconductor quantum dots inside photonic crystal, micropillar or microdisk resonators. We review the progress so far in obtaining true quantum-optical strong-coupling effects in semiconductors. We discuss the recent results on vacuum Rabi splitting with a single quantum dot, emphasizing the differences from quantum-well systems. Finally, we propose nonlinear tests for the true quantum limit and speculate about applications in quantum information devices.

G. KHITROVA[1]*, H. M. GIBBS[1], M. KIRA[2], S. W. KOCH[2] AND A. SCHERER[3]

[1]Optical Sciences Center, The University of Arizona, Tucson, Arizona 85721-0094, USA
[2]Department of Physics and Material Sciences Center, Philipps-University, Renthof 5, D-35032 Marburg, Germany
[3]Electrical Engineering, California Institute of Technology, Pasadena, California 91125, USA
*e-mail: galina@optics.arizona.edu

The ability to control the spontaneous emission of a quantum dot (QD) in a cavity allows the study of the regime of cavity quantum-electrodynamics (QED)[1,2]. Semiconductor structures offer the unique capability of permanently positioning a QD in the middle of a nanocavity. This review describes the history of realizing vacuum Rabi splitting (VRS) in the single-QD (SQD) regime, including the mechanisms involved, the essential parameters of the QDs and microcavities that have enabled successful realizations of SQD VRS, and the criteria that must be satisfied for the realization of genuine quantum behaviour, where one photon can control the transmission or reflection of a subsequent second photon. The true strong coupling regime is fascinating, as it allows nonlinear quantum optics experiments to be done with as few as two photons, control of the direction of emission or phase of one photon with another, the observation of single-atom lasing[3], the study and exploitation of quantum entanglement, and exploration of the boundary between classical and quantum physics[4–11].

If the coupling strength between two same-energy oscillators exceeds the mean of their decay rates, then the coupled system has two eigenenergies — that is, their states split. VRS occurs when one of the oscillators consists of a two-level atom or QD, and the other is that of a small-volume high-quality (high-$Q$) cavity. The name comes about because the VRS is numerically equal to twice the product of the transition dipole moment and the vacuum field arising from the root-mean-square of the vacuum fluctuations (zero-point energy of half a photon energy in the cavity mode). The term VRS is also used when the matter involves more than a single oscillator; for example, there is VRS due to many atoms or to a quantum well (QW). A simple way to understand VRS is to insert the QD or QW absorption and refractive index into the formula for the transmission of a Fabry–Perot interferometer; the transmission becomes double-peaked if the absorption is strong and narrow enough.

When such splitting takes place in a many-atom system, its behaviour is classical — removing one atom or absorbing one photon has little effect. However, if the VRS arises from the well-isolated transition of a single atom or SQD, then the VRS is a fundamentally quantum phenomenon — removing the SQD eliminates the splitting altogether — and is referred to as the strong coupling regime of VRS. Absorption of a single photon in this regime also has a profound effect, and causes the positions of the transmission peaks for a subsequent probe photon to shift considerably in energy. These single-photon changes can be used to make quantum gates. By adjusting the cavity decay rate to be much larger than the QD transition dephasing rate, the strong coupling can be used to emit a single photon on demand (when the system is pulse excited) with the photons indistinguishable from each other because the emission is deterministic (the same each time). All previous SQD sources of single photons have operated in the weak coupling regime of irreversible emission, but strong coupling is a reversible process that can be used to transfer quantum information between QDs and photons in a coherent manner. A, SQD VRS system can be prepared in a state where the coupled-system wavefunction must be written as a superposition of two possibilities: excited QD and

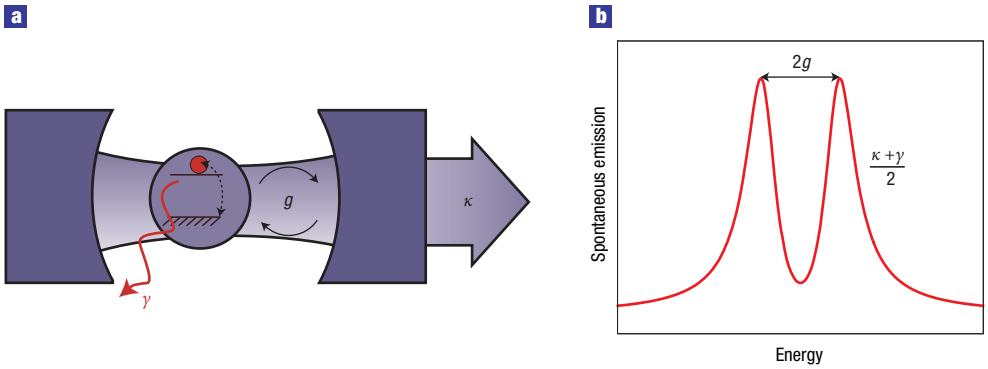


**Figure 1** Vacuum Rabi splitting using an atom or dot in a small-volume cavity. **a**, Schematic of a single two-level atom with dephasing rate $\gamma$ coupled to a cavity with photon loss rate $\kappa$ by coupling strength $g$. **b**, VRS spectrum for zero atom-cavity detuning.

no photon in the cavity, and an unexcited QD and one photon in the cavity. Such entanglement has potential for teleporting the quantum state (for example, spin up or down of a charged QD) in one cavity to another cavity far away. Quantum phase gates, turnstiles of indistinguishable single photons, and quantum-state transfer devices are enabling components for quantum information science.

In planar QD or QW structures, only 1–2% of the light exits because of the large difference between the refractive indices of the semiconductor and air. In spite of the fact that a single photon can be emitted in any direction and consequently be lost in the substrate, recent experiments have successfully detected emission from a single stationary dot[12,13], and shown that two photons are never emitted at the same time (antibunching[14]). The use of cavity effects can improve this situation dramatically, as researchers who were working on the development of single-photon-on-demand sources soon realized. Having an SQD embedded in a three-dimensional (3D) nanocavity both directs the emission into a single mode and reduces the emission lifetime due to the Purcell effect[15] — that is, the decrease in the dot's spontaneous emission lifetime that is caused by the location of the dots at the antinode of a cavity with a small volume $V$ and high quality factor $Q$[16,17]. The faster emission is desirable because it makes the photon-on-demand source more deterministic and reliable. The natural length of a semiconductor vertical-cavity surface-emitting laser (VCSEL) was already very short; as the Purcell effect scales as $Q/V$, an increase in $Q$ along with transverse confinement already reduced the spontaneous emission lifetime by a factor of five for QDs in resonance with the cavity mode, even though they were spatially distributed randomly[16].

By decreasing $V$ and increasing $Q$, the coupling is restricted principally to one mode of the electromagnetic field. To resolve the occurrence of single-atom VRS[18,19], the linewidths (ideally, $[\kappa+\gamma]/2$ for zero detuning) of the coupled system resonances have to be narrower than the splitting $2g$ — that is, twice the atom-field coupling strength $g=\mu E_{\mathrm{vac}}/\hbar$ (see Fig. 1). Here $\gamma$ and $\kappa$ are the homogeneous decay rates of the matter polarization and the light in the cavity, respectively, and $\hbar$ is the reduced Planck constant. The dipole moment of the QD is $\mu$, and $E_{\mathrm{vac}}=[\hbar\omega/(2\varepsilon_0 V)]^{1/2}/n$ is the so-called vacuum-field amplitude; $\varepsilon_0$ is the permittivity of free space, $\hbar\omega$ is the photon energy, where $\omega$ is the angular frequency of light, $V$ is the volume that the cavity-mode mostly occupies, and $n$ is the index of refraction of the non-resonant semiconductor. As $E_{\mathrm{vac}}$ scales with $1/\sqrt{V}$, it is essential to enhance $g$ by reducing $V$. These three basic radial frequencies $g$, $\gamma$, and $\kappa$ can be used to define the different regimes of atom-light coupling. In the weak coupling regime ($g<\gamma,\kappa$), the cavity Purcell effect[15] can either enhance or inhibit the decay rate of irreversible spontaneous emission if $g$ is large enough. On the other hand, if $g>\gamma,\kappa$, this is in the regime of true strong-coupling, and the quest for this in semiconductors is the focus of this review.

The spontaneous emission spectrum for a two-level system coupled to the single mode of a cavity (described by the Jaynes–Cummings[20] hamiltonian) has been derived by solving the corresponding master equation for the density matrix of the coupled system[21–23], an example of which is shown in Fig. 2. It is obvious that increasing $Q$ broadens the line — that is, the radiative emission is faster. However, the emission wavelength is less well determined with the eventual onset of VRS, which causes the emission to exhibit two peaks. In the low-$Q$, weak-coupling regime, the emission spectrum reduces to a single lorentzian line; the total linewidth $\gamma$ increases linearly: $\gamma=\gamma_{\mathrm{dot}}+\gamma_{\mathrm{enh}}$, where $\gamma_{\mathrm{enh}}=4g^2/\kappa=F_{\mathrm{P}}\gamma_0$ is the Purcell enhanced rate ($F_{\mathrm{P}}$ is the Purcell factor), $\gamma_{\mathrm{dot}}=\gamma_{\mathrm{nonrad}}+\gamma_0$, $\gamma_{\mathrm{nonrad}}$ is the dot's non-radiative dephasing rate, and $\gamma_0$ is the radiative decay rate of the dot outside the cavity. But as the coupling to a cavity with $\kappa>\gamma$ increases, $\gamma$ increases even faster than $F_{\mathrm{P}}\gamma_0$; the computed linewidth (solid curve) exceeds the linear Purcell enhancement (dashed line) as reported for an InAs dot in a photonic crystal cavity[24] ($Q=970$ hollow point in Fig. 2b). In that experiment radiative broadening dominated: $\gamma$ became four times larger than $\gamma_{\mathrm{dot}}$ which in turn was roughly a factor of 10 larger than $\gamma_0$, similar to the ratio for InGaAs QWs[25].

The first successful investigations into atomic cavity QED involved passing individual atoms of an atomic beam through a resonant microwave cavity one-by-one, with each new atom interacting with the field left by the atoms that preceded it. Cavity QED with semiconductor dots is topologically very different — it involves locating a single stationary

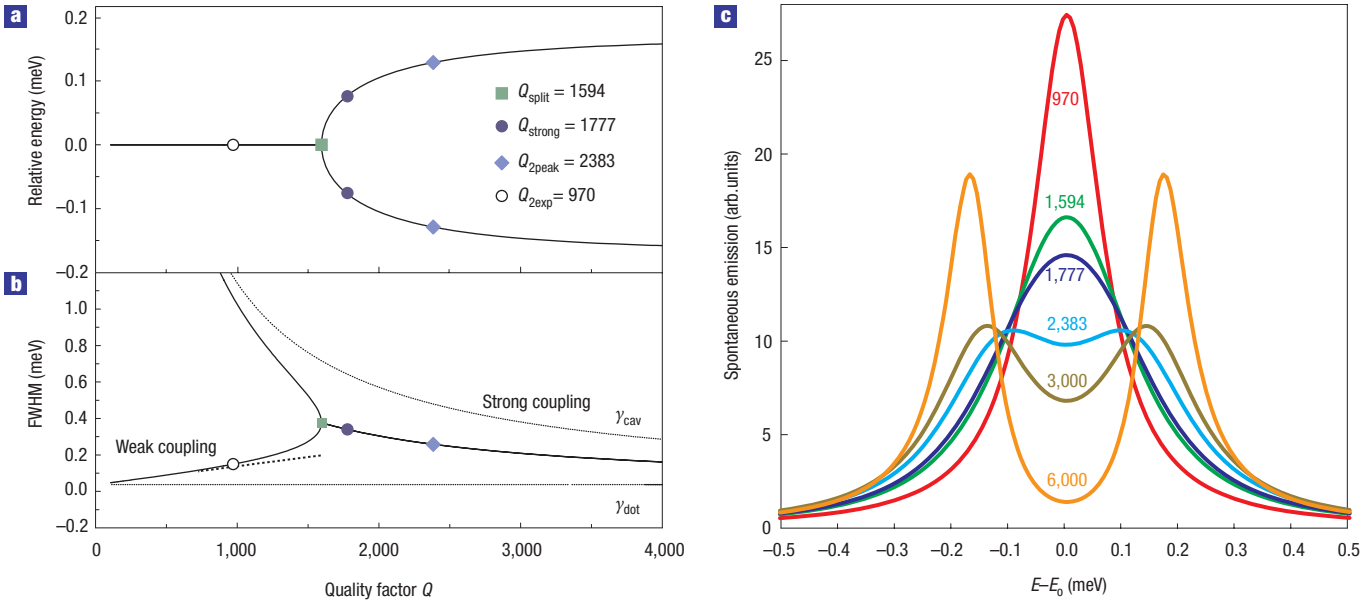


**Figure 2** Illustration of the transition from Purcell enhancement of two-level-atom spontaneous emission all the way to vacuum Rabi splitting. The transition shows the ability to overcome non-radiative broadening by cavity enhancement. Here we assume the behaviour of a QD can be approximated by a two-level system. **a**, Eigenenergies, **b**, linewidths, and **c**, spectra for $E_{dot} = E_{cavity} = E_0 = 1.1424$ eV. In the transition region for $Q$ increasing towards $Q_{split}$, the eigenenergies of the QD and nanocavity are degenerate and the linewidths approach each other; for $Q > Q_{split}$, the eigenenergies split and the linewidths are equal. In the strong-coupling limit, $2g \gg (\kappa + \gamma_{dot})/2$, the spectrum becomes a doublet, split by $\Omega_R = 2g$, with equal linewidths given by $(\kappa + \gamma_{dot})/2$. There is a smooth transition from the limiting cases, that is, from a single lorentzian to double-peaked structure. The commonly used condition for strong coupling, $2g \geq (\kappa + \gamma_{dot})/2$, is where the spectrum becomes somewhat flat-topped as shown by the $Q_{strong} = 1{,}777$ curve. Also shown are curves for $Q_{2peak} = 2{,}383$ for the clearly resolved case $\Omega \geq (\kappa + \gamma_{dot})/2$, where $\Omega$ is the actual splitting, which may be less than $2g$ because of broadening. These plots depend on only two parameters, namely $\gamma_{dot}/2\pi = 9$ GHz and $2g/2\pi = 82$ GHz; these values from ref. 24 are similar to those in Fig. 3.

dot within a cavity. This removes many of the variables associated with the atomic beam approach and enables many QED experiments to be carried out on the same object. Recently, however, atomic investigators have come close to realizing a similar situation by trapping an atom inside a cavity (though with the inevitable trade-off of reducing $g$ when increasing $V$ to make room for the trap). Coincidentally, the first observation of VRS due to a relatively stationary trapped atom[26] occurred in the same year as VRS with an SQD[27–29]. The essential advantage of studying cavity QED using atomic systems is their inherent simplicity; consequently their behaviour and the parameters that control this behaviour are well understood. The QD cavity QED problem is both challenging and exciting because many aspects are not yet well understood. For example, the QDs used to see SQD VRS in the linear regime are rather large, that is, if excited strongly they can contain many carriers and may even be charged. Is the transition coupled to the nanocavity sufficiently isolated that the SQD VRS system can indeed be used for the quantum information manipulations and devices mentioned above?

In this review, we focus on the regime of two-peak VRS. Any isolated resonance coupled to a single-mode cavity produces two transmission peaks if its absorption is strong and sharp enough[30]. Indeed, when a single QW was grown in the centre of a VCSEL, two-peak VRS was observed. As a semiconductor is much harder to understand and model, there were misconceptions about what was really seen. That is, was the effect quantum mechanical and directly analogous to single-atom VRS, or was it semiclassical, arising from many-atom VRS with the splitting multiplied by the square root of the number of atoms? To unravel the physics of QW VRS it was essential to conduct careful nonlinear experiments to determine the number of photons required to change the behaviour of the coupled system, and to compare this behaviour with a realistic theory — and it will be for QD VRS as well.

## VACUUM RABI SPLITTING WITH AN SQD

Figure 3 summarizes the three recent experiments[27–29] demonstrating SQD VRS and compares them with VRS due to a single trapped Cs atom[26]. Achieving SQD VRS required many years of effort. That strong coupling with a single interface-fluctuation-QD should be achievable in a pillar microcavity was predicted many years ago[22,31–34], and more recently using an InAs self-organized dot in a photonic crystal microcavity[35]. A semiconductor nanocavity with a small volume and high $Q$ is needed not only for SQD VRS, but also for low-threshold lasers and Purcell-enhanced photon emitters. Also, QDs are promising for some applications such as confining carriers to reduce the threshold and providing gain. Single-QD VRS would not have been seen without the great progress in QD growth and microcavity

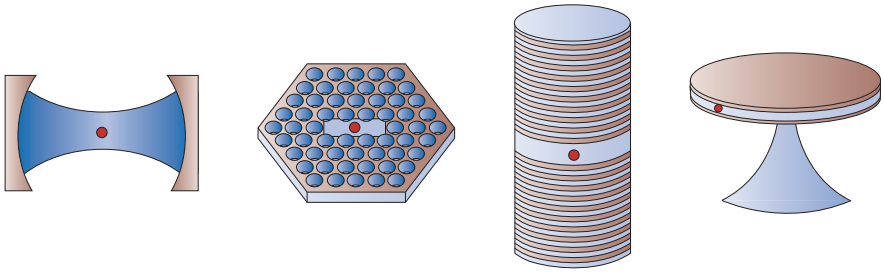

| **Cavity** | Length = 42.2 μm: Width = 23.4 μm: | Photonic crystal slab | Micropillar | Microdisk |
|---|---|---|---|---|
| $\lambda$ (nm); E (eV) | 852.4; 1.45 | 1,182; 1.32 | 937; 1.32 | 744; 1.66 |
| $Q$ | $4.4 \times 10^7$ | 6,000 | 7,350 | 12,000 |
| $V$ ($\mu m^3$) | $18{,}148 = 3 \times 10^4(\lambda/n)^3$ | $0.04 = (\lambda/n)^3$ | $0.3 = 16(\lambda/n)^3$ | $0.07 = 8(\lambda/n)^3$ |
| $F_P = \frac{3Q\lambda^3}{4\pi^2 n^3 V}$ | 114 | 441 | 36 | 125 |
| $\kappa/2\pi$ (GHz) | 0.008 | 42 | 44 | 34 |
| **Oscillator** | Trapped Cs atom | InAs QD | $In_{0.3}Ga_{0.7}As$ QD | GaAs QD |
| Size | $d = 0.54$ nm | $d < 25$ nm | $30 \times 100$ nm$^2$ | $d = 44$ nm |
| $\mu$ (D) | 8 | 29 | 60 | 92 |
| $\gamma_o/2\pi$ (GHz) | 0.005 | 0.088 | 0.76 | 3.6 |
| $\gamma/2\pi$ (GHz) | 0.005 | 22 | 18 | 68 |
| **VRS** | | | | |
| $2g/2\pi$ (GHz) | 0.068 | 41 | 39 | 196 |
| VRS/linewidth | 5 | 1.3 | 0.7 | 2.2 |

**Figure 3** Comparison of systems exhibiting vacuum Rabi splitting using a single oscillator: a single trapped atom[26] or a single QD in a photonic-crystal-slab nanocavity[28], in a micropillar[27], or a microdisk[29]. The values of VRS/linewidth are taken from the published VRS plots, so they sometimes differ from the ideal $2g/[(\kappa+\gamma)/2]$; in this figure $\gamma_{dot}$ is replaced by $\gamma$.

etching techniques largely driven by these technological goals.

## MICROCAVITIES

The great appeal of micro-QD and nanocavities is that they can be easily and monolithically fabricated, which in turn increases their suitability for large-scale integration into more-complex arrays and circuits. Almost every type of microcavity structure[36] has been considered in the quest for SQD VRS, including micropillars, microdisks, microspheres[36–38], photonic-crystal-slab nanocavities, and even an external mirror of very small radius of curvature[39,40].

In a micropillar device, optical confinement in the axial (vertical) direction is achieved in the same way as is achieved in a conventional planar microcavity — that is, with two Bragg-mirrors facing each other (which can lead to $Q$-factors as high as 5,000-10,000, ref. 41) — and in the radial (horizontal) direction by total internal reflection at the etched cylinder side walls[42]. One advantage of a micropillar cavity is that it emits light in the axial direction, which makes optical access to it with a microscope objective relatively simple.

Microdisk devices[43], on the other hand, confine light using total internal reflection in all three directions, which can support whispering-gallery modes that exhibit $Q$-factors exceeding 10,000. The direction of emission from a microdisk is usually not as well defined as it is for a micropillar, but can be made so using side coupling by an optical fibre taper — though this too involves a trade-off as $Q$ decreases with increased loading as the fibre is brought closer[44]. Early photonic-crystal cavities were attempts to combine a planar microcavity in the axial direction and a photonic crystal in the radial direction, but etching such thick structures yielded very low $Q$-factors. The first breakthrough was achieved through the use of a suspended slab to provide confinement by total internal reflection in the axial direction. Thereafter, $Q$-factors of order 1,000 were rapidly realized, leading in turn to the observation of lasing, first with QWs[45] and subsequently with QDs[46] as a means of achieving optical gain. The second breakthrough came when the geometric arrangement of the holes was modified[47], enabling empty-cavity $Q$-factors to jump to almost 50,000 in Si[47] (now close to 1,000,000)[48] and those of GaAs-based cavities to 20,000[28,49]. The design of the nanocavity of the photonic-crystal slab determines whether the emission occurs primarily in the plane, as desired for integrated optical circuitry, or perpendicular to the plane, convenient for single-cavity experiments. Note that the photonic-crystal-slab nanocavity is the only microcavity in Fig. 3 that has a volume of $(\lambda/n)^3$ or

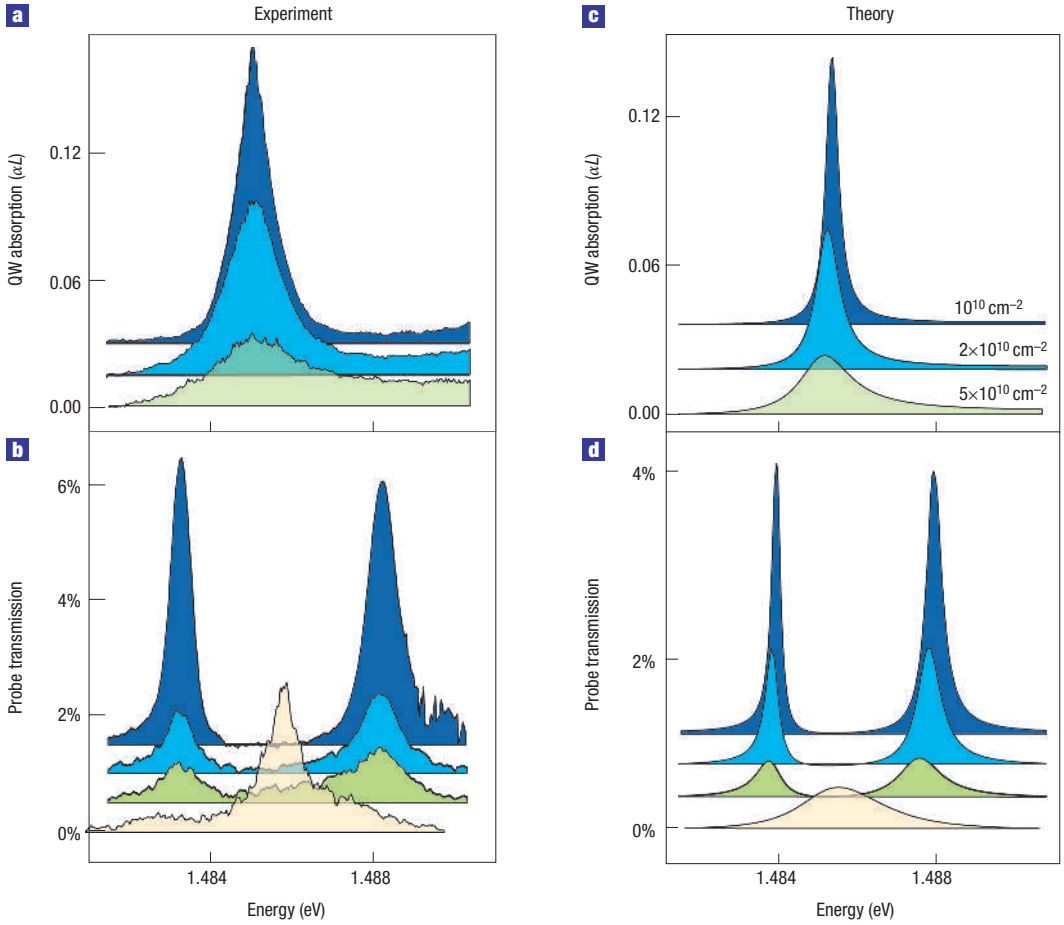


**Figure 4** Comparison of experimental and theoretical VRS for QWs positioned inside a planar microcavity. **a**, Experimental probe transmission spectra with increasing pumping at 1.575 eV for excitonic absorption of 20 QWs like those in the microcavity; the excitation level increases from top to bottom as the shading becomes lighter. **b**, The experimental probe transmission for two QWs inside the microcavity. Clear double-peaked VRS is observed. Kramers–Kronig transfer-matrix microcavity calculations using the nonlinear data in **a** indicate that colours in frame **a** and **b** have matching excitation levels. Stronger pumping in **b** results in lasing at a wavelength close to the light yellow peak. **c**, Microscopically computed bare QW absorption corresponding to the experiments. **d**, By using the microscopically evaluated susceptibility in a transfer-matrix calculation, we obtain the probe transmission of the QW microcavity for increasing carrier density (from top to bottom as the shading becomes lighter). This semiclassical analysis fully explains the experimental VRS as well as the collapse to a single resonance (light yellow). Data from ref. 79.

less, permitting the observation of SQD VRS with a much smaller QD.

## QDS

Obviously SQD VRS is as dependent on growing a QD with a large dipole moment and small dephasing, as on fabricating a small-volume cavity with high $Q$. Three-dimensional confinement of a semiconductor was first seen and correctly interpreted as a particle in a box ('artificial atom') when small semiconductor nanocrystals grew in glass[50,51]. The principal types of QDs considered for strong coupling have been the interface-fluctuation QD and the self-assembled QD. The interface-fluctuation QD is a 3–6 nm GaAs single QW grown by molecular beam epitaxy, with growth interruptions at one or both of the interfaces between the GaAs well and the AlAs or AlGaAs barriers[52,53]. This technique yields islands that are one monolayer thicker than their surroundings and have a typical lateral size of 40–50 nm[54,55], much larger than the bulk exciton radius. Because of the big lattice mismatch between GaAs and InAs, self-assembled dots form when strain destroys 2D growth after more than 1.75 monolayers of InAs are deposited on top of GaAs[12,56–58]; usually a self-assembled dot is 3–4 nm high with a 10–25 nm base.

The ability to quantum-confine a semiconductor allows the investigation of quantum mechanics at the fabrication–technological level. Clearly, QWs not only produced cutting edge research but greatly improved technology. Similar advances are in progress in the QD field. Many of the QD milestones, such as their growth and the spectroscopy of a single dot, are summarized in reviews[59,60]. Narrow homogeneous linewidths were observed for both an interface-fluctuation QD (23 μeV)[13] and a self-assembled QD[61,62] (1.8 μeV)[63], under conditions of low excitation to avoid broadening by carriers moving around. The dipole moment of an interface-fluctuation QD was predicted to be very large[22,34,64] (50–100 D), as verified by Rabi flopping[65] and direct absorption[66]. The smaller size of an InAs QD results in a smaller dipole moment ($\mu = 25$–$35$ D), which can be extracted from ensemble measurements of the lifetime $\tau$ (1–2 ns) using[64] $1/\tau = n\omega_0{}^3\mu^2/3\pi\varepsilon_0\hbar c^3$, where $\omega_0$ is the transition angular frequency, and $c$ is the speed of light in a vacuum. An InAs self-assembled QD[14,67] and even a GaAs interface-fluctuation QD[68] are sufficiently like a single atom that antibunching has been seen with the help of a filter that transmits light only at the ground-state transition.

## SQD VRS

Achieving SQD VRS would be much easier if one isolated QD could be placed in the cavity antinode (spatial coincidence) with a transition wavelength coinciding with the cavity resonance (spectral coincidence). In reality, all three of the successful

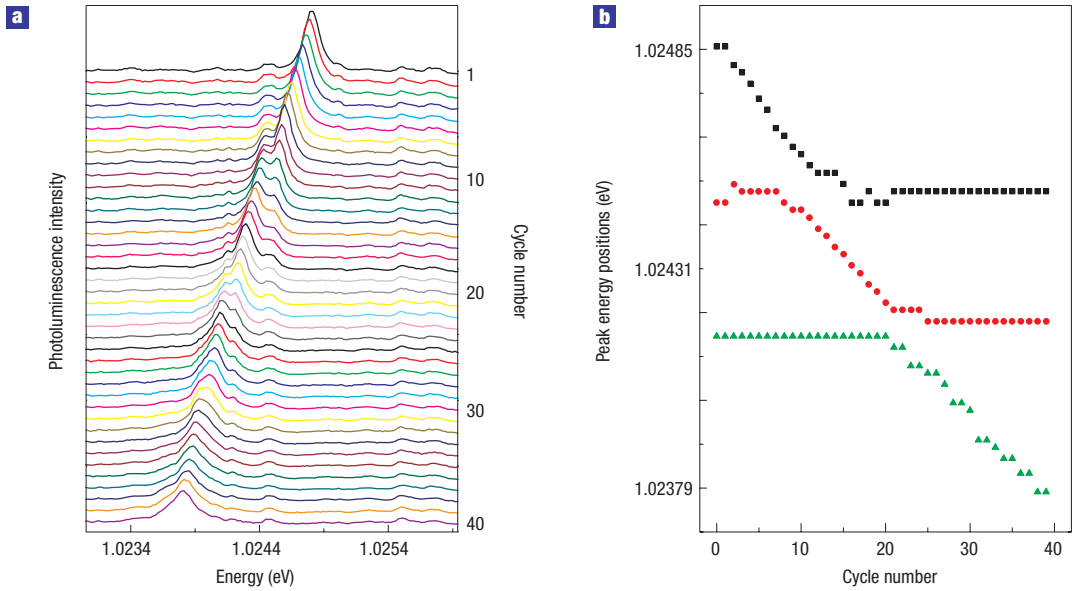


**Figure 5** SQD VRS using Xe condensation. **a**, photoluminescence spectra at 25K with low-power continuous-wave excitation (1.2 μW; 10 s exposure time) at 1.610 eV versus detuning controlled by condensing Xe in increments of 0.46 torr each cycle. **b**, Peak positions in the spectra versus cycle number. Two anticrossings (the signature of SQD VRS) occur between the nanocavity mode and two distinct SQDs. Data from ref. 96.

SQD VRS experiments had to look at many microcavities in search of these two coincidences, and temperature scanning of the QD transition by $\cong$1 meV through the cavity resonance was used to map out the anticrossing. To reduce the search problem, high dot densities (400 $\mu m^{-2}$) are often used. This may be detrimental; the ensemble absorption of a single layer of dots of this density reduces the $Q$-factor of the photonic-crystal-slab nanocavity in Fig. 3 from the empty-cavity value of 20,000 down to 6,000[49].

Finding an SQD in a high-$Q$, small-volume nanocavity is not unique to SQD VRS; it is also needed to see Purcell enhancement of spontaneous emission. The search for SQD VRS benefitted from that earlier work. A landmark experiment was the enhancement of the spontaneous emission rate by a factor of up to five for the ensemble of QDs in resonance with one mode of a micropillar ($Q = 2{,}250$, diameter 1 μm)[16]. A transition of a single self-assembled dot was temperature-scanned through the mode ($Q = 6{,}500$) of a 5-μm-diameter microdisk[69] (measured maximum $F_P$ of 6). Extensions of that early research have resulted in high collection efficiency for weak-coupling cavity-QED emitters of single photons using micropillar[70–72] and photonic-crystal-slab[73] cavities.

The most significant difference between the three SQD VRS experiments in Fig. 3 is the size of the QD. The larger the QD, the larger $\mu$, so SQD VRS can be seen with a larger $V$. The larger $V$s of the micropillar and microdisk cavities were compensated for by increasing the size of the QD to increase $\mu$. This also explains the big differences in $\gamma_0$ in Fig. 3, as it is proportional to $\mu^2/\lambda^3$. Clearly the larger the QD, the larger $g$ and the more impressive the splitting-to-linewidth ratio. But if the QD becomes too big, it is effectively a QW microcavity system that is semiclassical, not quantum; see the next section. The near-minimum-volume nanocavity of the photonic-crystal slab has the decided advantage of giving the largest $E_{vac}$ with a very high $Q$, so it has the best chance for SQD VRS that is truly strong coupling. Absorption of a single photon would change the absorption spectrum for the next photon, and climbing of the Jaynes–Cummings ladder would be possible. However, it should be pointed out that even the largest dot in Fig. 3 satisfies the simplest condition for seeing ladder climbing, namely that the transition be relatively isolated: the VRS is much smaller than the energy difference to the nearest transition.

The fact that the position of the QD is fixed means that the strength of the coupling $g$ is time-independent. Of course, there are technological challenges to improve $Q$ of these nanodevices and the optical coupling in and out of them by a nearby waveguide or fibre; see for example refs 36,44,47,48,74. Clearly, the photonic-crystal slab lends itself to waveguide interconnections between VRS devices and to operation at fibre wavelengths.

## QW VRS: NON-PERTURBATIVE, SEMICLASSICAL REGIME

The curious development of the field of semiconductor microcavities often produced results different from the original goals. In the 1980s, excitement in the fields of optical computing and switching pushed semiconductor bistable etalons to their extremes, but now it is the VCSEL, not parallel optical computing, that impacts the economy. Predecessors to the VRS microcavity were the bistable nonlinear etalon[75], the monolithic Fabry–Perot etalon[76], and the VCSEL[77], consisting of a QW inside a spacer between two distributed feedback mirrors. When a VCSEL was designed and grown for low-temperature operation, the QW absorption became much narrower (no phonon broadening), and the cavity resonance remained the same; immediately, an anticrossing scan revealed two reflection dips — the first semiconductor VRS[78]. In the beginning, it was not clear in which regime of

light-matter coupling the system was operating. The growth of a sample with InGaAs QWs with narrow absorption linewidths (Fig. 4a) resulted in VRS with a larger splitting-to-linewidth ratio (Fig. 4b)[32]. The obvious experiment was to figure out if the semiconductor community had made a huge step, ending up in the true strong-coupling regime where absorption of a single photon makes a difference. The nonlinear absorption of the cavityless QWs (Fig. 4a) as well as the transmission of the VRS microcavity containing the same QWs (Fig. 4b) were measured as a function of carrier density generated non-resonantly[79]. The microcavity transmission was then analysed theoretically using the semiclassical transfer-matrix approach, where the microscopically computed QW susceptibility (Fig. 4c) input enters as a function of excitation level[79]. As the computed (Fig. 4d) and measured nonlinear transmissions agreed well, one had to conclude that the QW VRS is semiclassical, corresponding to many-atom VRS[80–82]. Following the nomenclature of the atomic physics community[83], we refer[32] to this coupling as non-perturbative normal-mode coupling to distinguish it from true strong-coupling.

### SATURATION NUMBER OF PHOTONS

Can one determine just how far a QW VRS microcavity is from true strong-coupling where quantized-field effects could be seen? One way to determine the number of absorbers in a container is to count how many photons need to be absorbed to reduce the absorption in half. Using a beam diameter of 50 μm, it took 200,000 photons to saturate the single QW absorption and appreciably alter the VRS[32]; see light-blue curves in Fig. 4. Using a 2-μm-oxide-aperture 3D microcavity, 300 photons still had to be absorbed[84]. Using several aperture sizes, it was determined that 90 photons per $\mu m^2$ must be absorbed; this number extrapolates to a single photon for a QW diameter of about 100 nm, suggesting that a large-diameter SQD could exhibit VRS. Of course, the cavity mode diameter cannot be that small, so the VRS will be much smaller ($\sim$1/100), with a very large SQD than with a QW filling the mode cross-section, as shown above. Similar nonlinear experiments need to be performed to see how many photons are needed to saturate SQD VRS, that is, is the QD in each of the microcavities small enough to place the coupled system in the regime of true strong-coupling? Clearly, increasing the SQD size increases the splitting, but in the limit the system becomes a semiclassical QW 3D microcavity.

### LUMINESCENCE

As long as the transmission is double-peaked, the microcavity also emits two-peaked photoluminescence after non-resonant excitation[85]. It is the very large QW excitonic absorption that results in the splitting in the transmission, reflection, and absorption of the QW/cavity-coupled system. The same light-matter coupling determines the spectral resonances regardless of how the spontaneous emission is initiated. Thus, the presence of double peaks in the photoluminescence spectrum does not identify the source of the light. In particular, the question might be asked if this double-peaked spectrum implies that the emission has its origin in exciton populations? It can be understood that the answer is no, at least in III–V QWs, by again considering the case of cavityless QWs[86–91]. Even though not everyone[92] agrees on all the details of the analysis of the QW 1*s* photoluminescence for very low temperatures and densities, it is by now established that an electron–hole plasma can emit at the 1*s* exciton resonance — as first predicted by the microscopic theory[86] — and that indeed the 1*s* photoluminescence is almost entirely coming from the plasma at densities higher than 200 $\mu m^{-2}$ for which the peak exciton absorption is reduced by only 25% and the QW VRS is hardly affected. Thus, one might guess that the photoluminescence from a non-resonantly excited QW microcavity may also be coming from the plasma population. The presence of VRS does affect the photoluminescence spectrum by determining whether the emission is enhanced or inhibited at any given frequency. But it does not determine the origin of the emission, that is, which material excitations store the energy that will be released in a recombination process.

Indeed, the first application of a quantum theory for photoluminescence from an interacting carrier system in a III–V semiconductor explained the non-resonantly pumped VRS microcavity experiments, where, with increased pumping, the upper branch emission overtook and far surpassed the lower branch emission[93]. The computations reproduced all of the features of this 'boser' emission[94,95], including the low-density double-peaked emission around the exciton peak; the dramatic overtaking was simply the result of the nonlinear effects of the microcavity modes on the plasma emission. As the overtaking occurred close to the collapse of the VRS into the weak coupling regime, the relevant density range was too high for excitons to exist, thus explaining the excellent agreement with a theory that left them out. Only at very low densities and low temperatures can one expect the photoluminescence from a non-resonantly excited VRS microcavity to have appreciable contributions from an exciton population.

## WHAT'S NEXT FOR SQD VRS?

### DETERMINISTIC SPATIAL AND SPECTRAL COINCIDENCES

Tuning with temperature is not completely satisfactory — the dot behaviour itself changes due to acoustic phonon broadening with increased temperature. Recently, a new technique for tuning[96] has been developed, namely condensation of Xe; see Fig. 5. The solid Xe coating the slab and hole walls has a higher refractive index than in vacuum and shifts the nanocavity mode to lower energy. This technique gives an enhanced scan range (4 meV) and allows the QD to be kept at low temperature. It will be interesting to see if it works for other types of cavities.

Even better than having a layer of dots requiring scanning to find one positioned favourably within the field distribution, would be to have a single dot around which a cavity is constructed and then tuned into resonance. Progress in that direction has been reported, but VRS has not been achieved: a photonic-crystal nanocavity was fabricated around a particular QD, and etching was used to scan the nanocavity peak digitally in 3-nm steps[97]. Clearly, techniques for the deterministic placement of an SQD in a field antinode and for making the QD and cavity resonances degenerate will greatly accelerate progress.

## DEPHASING

Atomic-cavity QED has the simple advantage that each atom is always the same with very few dephasing events within the relevant timescales; as a result, the system contains dominantly only pure radiative broadening $\gamma_{\mathrm{rad}} = \gamma_0$. In contrast to this, the total dephasing $\gamma$ is dominantly non-radiative $\gamma \approx \gamma_{\mathrm{nonrad}}$ for current SQD samples. But the semiconductor systems are not so bad after all; in both quantum wells and dots, $\gamma/\gamma_{\mathrm{rad}}$ is often about ten[25] such that the common misconception that dephasing is a big problem in semiconductors is not true. As can be seen from Fig. 3, even though the dephasing rate is much larger than the atomic one, so is the Rabi splitting because of the very large dipole moment — giving a similar impressionistic picture of the splitting-to-linewidth ratio for the trapped-atom and QD cases. As a clear benefit for the dots, they can be grown and tailored as required. It is both a curse and a blessing, but clearly incredible progress was made for single QWs — a thick GaAs well has been grown[98] with $\gamma/\gamma_{\mathrm{rad}}$ close to 1. The same should be done with single dots, which could lead to a huge number of cavities on a single chip all interconnected by photonic-crystal waveguides.

## SECOND PHOTON EFFECTS

In a true strong-coupling system, nonlinear optics occurs with only two photons[4,10,99,100]. In fact[11], the transmission or reflection of a cavity can be controlled by absorption of a single photon. It will be important to perform nonlinear experiments to prove that each QD/nanocavity structure behaves as a true strong-coupling system. The smaller the QD, the farther apart are its quantized energy levels and the more likely it will exhibit quantized-field effects such as climbing the Jaynes–Cummings ladder when more photons are added to the cavity mode[101,102]. For each light mode, we have the number states $|n\rangle$, often referred to as photon states, which represent the quantized light field. In the true strong-coupling regime, each $|n\rangle$ state provides an individual minimum splitting of $2g\sqrt{n}$; this constitutes the famous Jaynes–Cummings ladder. The ladder ground-state (unexcited atom and field vacuum state $|0\rangle$) is unsplit, the first rung of the ladder has VRS $2g$, the second rung has a larger splitting $2g\sqrt{2}$, and so on. Emission from the first to ground rungs is observed in Figs 3 and 5. The unequal splittings in the lower rungs are sometimes referred to as quantum Rabi splittings[10,102]. The only experimental evidence of higher rungs of the ladder is the increase in the Rabi oscillation frequency when the cavity was prepared in a state of one, two ... photons before an atom entered[102]. Quantized-field effects such as entanglement are best studied using the lowest few rungs. In contrast, high on the ladder, $n$ is very large and the splitting in states $|n\rangle$, $|n+1\rangle$, and $|n+2\rangle$ are almost identical, so transitions between them just give the Mollow triplet.

In this review, we have pointed out that a QW microcavity, even when etched into a micropillar of diameter 1 μm, operates in the semiclassical regime and will not exhibit ladder-climbing effects. A microcavity with a very large QD will not either. An open question is just how large can a QD be and still exhibit such effects? A QD is very different from an atom in that two units of excitation are above the ionization level of the QD; that is, a second rung level may have a decay channel not just to the first rung, but also to an ionized QD in a cavity with no photon. If a QD nanocavity is ever to exhibit controlled entanglement, a QD must be found that is atom-like enough that such competing incoherent processes do not destroy the desired coherent one. Another way to express the problem is to note that the Jaynes–Cummings ladder is true only for a two-level system, and the question remains: to what degree can a real QD be designed to approximate such a two-level system?

## QUANTUM INFORMATION DEVICES

Following a single-atom experiment, it is likely that a QD nanocavity will be operated as a continuous wave source of non-classical light, exhibiting antibunching (never more than one photon at a time) and a more uniform time spacing between photons (the bunching associated with an ordinary laser obeying Poisson statistics is almost entirely absent)[3,103,104]. A pulsed QD nanocavity could serve as a single photon turnstile that is more deterministic than one based on Purcell enhancement[105], that is, it will have less jitter and more nearly indistinguishable photons[97,106], and higher quantum efficiency[107]. Controlled quantum entanglement in a QD nanocavity could be used for quantum-state transfer where true strong-coupling serves as a bidirectional interface between semiconductor and photonic quantum states, as required in a quantum network[108,109].

There is every reason to believe that these solid-state implementations of single-oscillator VRS will be shown to exhibit true strong-coupling, opening up a rich vein of research on truly quantum effects with implications for quantum information science and fundamental quantum optics.

doi:10.1038/nphys227

## References

1. Berman, P. R. (ed.) *Cavity Quantum Electrodynamics* (Academic, Boston, 1994).
2. Haroche, S. & Kleppner, D. Cavity quantum electrodynamics. *Phys. Today* 24–30 (January, 1989).
3. McKeever, J., Boca, A., D. Boozer, A., Buck, J. R. & Kimble, H. J. Experimental realization of a one-atom laser in the regime of strong coupling. *Nature* **425,** 268–271 (2003).
4. Kimble, H. J. Strong interactions of single atoms and photons in cavity QED. *Phys. Scripta* **76,** 127–137 (1998).

5. Hood, C. J., Chapman, M. S., Lynn, T. W. & Kimble, H. J. Real-time cavity QED with single atoms. *Phys. Rev. Lett.* **80,** 4157–4160 (1998).
6. Ye, J., Vernooy, D. W. & Kimble, H. J. Trapping of single atoms in cavity QED. *Phys. Rev. Lett.* **83,** 4987–4990 (1999).
7. Nogues, G. *et al.* Seeing a single photon without destroying it. *Nature* **400,** 239–242 (1999).
8. Haroche, S. Entanglement, decoherence and the quantum/classical boundary. *Phys. Today* 36–42 (July, 1998).
9. Bertet, P. *et al.* A complementarity experiment with an interferometer at the quantum-classical boundary. *Nature* **411,** 166–170 (2001).
10. Raimond, J. M., Brune, M. & Haroche, S. Manipulating quantum entanglement with atoms and photons in a cavity. *Rev. Mod. Phys.* **73,** 565–582 (2001).
11. Birnbaum, K. M. *et al.* Photon blockade in an optical cavity with one trapped atom. *Nature* **436,** 87–90 (2005).
12. Marzin, J.-Y., Gérard, J.-M., Izraël, A., Barrier, D. & Bastard, G. Photoliminescence of single InAs quantum dots obtained by self-organized growth on GaAs. *Phys. Rev. Lett.* **73,** 716–719 (1994).
13. Gammon, D., Snow, E. S., Shanabrook, B. V., Katzer, D. S. & Park, D. Homogeneous linewidths in the optical spectrum of a single gallium arsenide quantum dot. *Science* **273,** 87–90 (1996).
14. Michler, P. *et al.* Quantum correlation among photons from a single quantum dot at room temperature. *Nature* **406,** 968–970 (2000).
15. Purcell, E. M. Spontaneous emission probabilities at radio frequencies. *Phys. Rev.* **69,** 681–681 (1946).
16. Gérard, J. M. *et al.* Enhanced spontaneous emission by quantum boxes in a monolithic optical microcavity. *Phys. Rev. Lett.* **81,** 1110–1113 (1998).
17. Bayer, M. *et al.* Inhibition and enhancement of the spontaneous emission of quantum dots in structured microresonators. *Phys. Rev. Lett.* **86,** 3168–3171 (2001).
18. Thompson, R. J., Rempe, G. & Kimble, H. J. Observation of normal-mode splitting for an atom in an optical cavity. *Phys. Rev. Lett.* **68,** 1132–1135 (1992).
19. Bernardot, F., Nussenzvieg, P., Brune, M., Raimond, J. M. & Haroche, S. Vacuum Rabi splitting on a microscopic atomic sample in a microwave cavity. *Europhys. Lett.* **17,** 33–38 (1992).
20. Jaynes, E. T. & Cummings, F. W. Comparison of quantum and semiclassical radiation theories with application to beam maser. *Proc. IEEE* **51,** 89–109 (1963).
21. Carmichael, H. J., Brecha, R. J., Raizen, M. G., Kimble, J. & Rice, P. R. Subnatural linewidth averaging for coupled atomic and cavity-mode oscillators. *Phys. Rev. A* **40,** 5516–5519 (1989).
22. Andreani, L. C., Panzarini, G. & Gérard, J. M. Strong-coupling regime for quantum boxes in pillar microcavities: Theory. *Phys. Rev. B* **60,** 13276–13279 (1999).
23. Goldstein, E. & Meystre, P. in *Spontaneous Emission and Laser Oscillations in Microcavities* (eds Yokoyama, H. & Ujihara, K.) 1–46 (CRC, New York, 1995).
24. Gibbs, H. M. in *Optics of Semiconductors and Their Nanostructures* (eds Kalt, H. & Hetterich, M.) 189–208 (Springer, Berlin, 2004).
25. Prineas, J. P. *et al.* Exciton-polariton eigenmodes in light-coupled $In_{0.04}Ga_{0.96}As$/GaAs semiconductor multiple quantum well periodic structures. *Phys. Rev. B* **61,** 13863–13872 (1994).
26. Boca, A. *et al.* Observation of the vacuum Rabi spectrum for one trapped atom. *Phys. Rev. Lett.* **93,** 233603 (2004).
27. Reithmaier, J. P. *et al.* Strong coupling in a single quantum dot-semiconductor microcavity system. *Nature* **432,** 197–200 (2004).
28. Yoshie, T. *et al.* Vacuum Rabi splitting with a single quantum dot in a photonic crystal nanocavity. *Nature* **432,** 200–203 (2004).
29. Peter, E. *et al.* Exciton photon strong-coupling regime for a single quantum dot in a microcavity. *Phys. Rev. Lett.* **95,** 067401 (2005).
30. Zhu, Y. *et al.* Vacuum Rabi splitting as a feature of linear-dispersion theory: Analysis and experimental observations. *Phys. Rev. Lett.* **64,** 2499–2502 (1990).
31. Khitrova, G. in *Quantum Optoelectronics, Postconference Edition of Technical Digest* 77–78 (Optical Society of America, Washington, 1999).
32. Khitrova, G., Gibbs, H. M., Jahnke, F., Kira, M. & Koch, S. W. Nonlinear optics of normal-mode-coupling semiconductor microcavities. *Rev. Mod. Phys.* **71,** 1591–1639 (1999).
33. Ell, C. *et al.* Toward quantum entanglement in a quantum-dot nanocavity. *IEEE LEOS Newslett.* **13,** 8–9 (1999).
34. Andreani, L. C., Panzarini, G. & Gérard, J. M. Vacuum-field Rabi splitting for quantum boxes in pillar microcavities. *Phys. Stat. Solidi A* **178,** 145–148 (2000).
35. Vučković, J. & Yamamoto, Y. Photonic crystal microcavities for cavity quantum electrodynamics with a single quantum dot. *Appl. Phys. Lett.* **82,** 2374–2376 (2003).
36. Vahala, K. J. Optical microcavities. *Nature* **424,** 839–846 (2003).
37. Lefevre-Seguin, V. & Haroche, S. Towards cavity-QED experiments with silica microspheres. *Mater. Sci. Eng. B* **48,** 53–58 (1997).
38. Fan, X., Palinginis, P., Lacey, S., Wang, H. & Lonergan, M. Coupling semiconductor nanocrystals to a fused-silica microsphere: a quantum-dot microcavity with extremely high Q factors. *Opt. Lett.* **25,** 1600–1602 (2000).
39. Raymer, M. G. *et al.* in *Frontiers in Optics/Laser Science XIX* WGG5 (Optical Society of America, Washington, 2003).
40. Cui, G. *et al.* A hemispherical, high-solid-angle optical micro-cavity for cavity-QED studies. Preprint at <http://arxiv.org/abs/quant-ph/0601046> (2006).
41. Stanley, R. P., Houdré, R., Oesterle, U., Gailhanou, M. & Ilegems, M. Ultrahigh finesse microcavity with distributed Bragg reflectors. *Appl. Phys. Lett.* **65,** 1883–1885 (1994).
42. Gérard, J. M. *et al.* Quantum boxes as active probes for photonic microstructures: The pillar microcavity case. *Appl. Phys. Lett.* **69,** 449–451 (1996).
43. McCall, S. L., Levi, A. F. J., Slusher, R. E., Pearton, S. J. & Logan, R. A. Whispering-gallery mode microdisk lasers. *Appl. Phys. Lett.* **60,** 289–291 (1992).
44. Srinivasan, K. *et al.* Optical loss and lasing characteristics of high-quality-factor AlGaAs microdisk resonators with embedded quantum dots. *Appl. Phys. Lett.* **86,** 151106 (2005).
45. Painter, O. *et al.* Two-dimensional photonic band-gap defect mode laser. *Science* **284,** 1819–1821 (1999).
46. Yoshie, T. O., Shchekin, B., Chen, H., Deppe, D. G. & Scherer, A. Quantum dot photonic crystal lasers. *Electron. Lett.* **38,** 967–968 (2002).
47. Akahane, Y., Asano, T., Song, B.-S. & Noda, S. High-Q photonic nanocavity in a two-dimensional photonic crystal. *Nature* **425,** 944–947 (2003).
48. Song, B.-S., Noda, S., Asano, T. & Akahane, Y. Ultra-high-Q photonic double-heterostructure nanocavity. *Nature Mater.* **4,** 207–210 (2005); *ibid* in *First Conf. Advances in Optical Materials* abstract IS17 (Elsevier, Oxford, 2005).
49. Hendrickson, J. *et al.* Quantum dot photonic-crystal-slab nanocavities: quality factors and lasing. *Phys. Rev. B* **72,** 193303 (2005).
50. Ekimov, A. I. & Onushchenko, A. A. Quantum size effect in three dimensional microscopic semiconductor crystals. *JETP Lett.* **34,** 345 (1981).
51. Efros, Al. L. & Efros, A. L. Interband absorption of light in a semiconductor sphere. *Sov. Phys. Semicond.* **16,** 772 (1982).
52. Zrenner, A. *et al.* Quantum dots formed by interface fluctuations in AlAs/GaAs coupled quantum well structures. *Phys. Rev. Lett.* **72,** 3382–3385 (1994).
53. Brunner, K., Abstreiter, G., Böhm, G., Tränkle, G. & Weimann, G. Sharp-line photoluminescence and two-photon absorption of zero-dimensional biexcitons in a GaAs/AlGaAs structure. *Phys. Rev. Lett.* **73,** 1138–1141 (1994).
54. Gammon, D., Snow, E. S., Shanabrook, B. V., Katzer, D. S. & Park, D. Fine structure splitting in the optical spectra of single GaAs quantum dots. *Phys. Rev. Lett.* **76,** 3005–3008 (1996).
55. von Freymann, G. *et al.* Level repulsion in nano-photoluminescence spectra from single GaAs quantum wells? *Phys. Rev. B* **65,** 205327 (2002).
56. Leonard, D. *et al.* Direct formation of quantum-sized dots from uniform coherent islands of InGaAs on GaAs surfaces. *Appl. Phys. Lett.* **63,** 3203–3204 (1993).
57. Moison, J. M. *et al.* Self-organized growth of regular nanometer-scale InAs dots on GaAs. *Appl. Phys. Lett.* **64,** 196–198 (1994).
58. Petroff, P. M., Lorke, A. & Imamoglu, A. Epitaxially self-assembled quantum dots. *Phys. Today* 46–52 (May, 2001).
59. Bányai, L. & Koch, S. W. *Semiconductor Quantum Dots* (World Scientific, Singapore, 1993).
60. Zrenner, A. A close look on single quantum dots. *J. Chem. Phys.* **112,** 7790–7798 (2000).
61. Kammerer, C. *et al.* Line narrowing in single semiconductor quantum dots: Toward the control of environment effects. *Phys. Rev. B* **66,** 041306 (2002).
62. Birkedal, D., Leosson, K. & Hvam, J. M. Long coherence times in self-assembled semiconductor quantum dots. *Superlattice Microstruct.* (special issue) **31,** 97–105 (2002).
63. Bayer, M. & Forchel, A. Temperature dependence of the exciton homogeneous linewidth in $In_{0.60}Ga_{0.40}As$/GaAs self-assembled quantum dots. *Phys. Rev. B* **65,** 041308 (2002).
64. Thränhardt, A., Ell, C., Khitrova, G. & Gibbs, H. M. Relation between dipole moment and radiative lifetime in interface fluctuation quantum dots. *Phys. Rev. B* **65,** 035327 (2002).
65. Stievater, T. H. *et al.* Rabi oscillations of excitons in single quantum dots. *Phys. Rev. Lett.* **87,** 133603 (2001).
66. Guest, J. R. *et al.* Measurement of optical absorption by a single quantum dot exciton. *Phys. Rev. B* **65,** 241310 (2002).
67. Becher, C. *et al.* Nonclassical radiation from a single self-assembled InAs quantum dot. *Phys. Rev. B* **63,** 121312 (2001).
68. Hours, J. *et al.* Single photon emission from individual GaAs quantum dots. *Appl. Phys. Lett.* **82,** 2206–2208 (2003).
69. Kiraz, A. *et al.* Cavity-quantum electrodynamics using a single InAs quantum dot in a microdisk structure. *Appl. Phys. Lett.* **78,** 3932–3934 (2001).
70. Moreau, E. *et al.* Single-mode solid-state single photon source based on isolated quantum dots in pillar microcavities. *Appl. Phys. Lett.* **79,** 2865–2867 (2001).
71. Pelton, M. *et al.* Efficient source of single photons: A single quantum dot in a micropost microcavity. *Phys. Rev. Lett.* **89,** 233602 (2002).
72. Vučković, J , Fattal, D., Santori, C., Solomon, G. S. & Yamamoto, Y. Enhanced single-photon emission from a quantum dot in a micropost microcavity. *Appl. Phys. Lett.* **82,** 3596–3598 (2003).
73. Englund, D. *et al.* Controlling the spontaneous emission rate of single quantum dots in a two-dimensional photonic crystal. *Phys. Rev. Lett.* **95,** 013904 (2005).
74. Scherer, A. *et al.* Photonic crystal nanocavities for efficient light confinement and emission. *J. Kor. Phys. Soc.* **42,** 768–773 (2003).
75. Gibbs, H. M. *Optical Bistability: Controlling Light with Light* (Academic, New York, 1985).
76. Jewell, J. L., Lee, Y. H., McCall, S. L., Harbison, J. P. & Florez, L. T. High-finesse (Al,Ga)As interference filters grown by molecular beam epitaxy. *Appl. Phys. Lett.* **53,** 640–642 (1988).
77. Jewell, J. L., Harbison, J. P. & Scherer, A. Microlasers. *Sci. Am.* 86–94 (November, 1991).
78. Weisbuch, C., Nishioka, M., Ishikawa, A. & Arakawa, Y. Observation of the coupled exciton-photon mode splitting in a semiconductor quantum microcavity. *Phys. Rev. Lett.* **69,** 3314–3317 (1992).
79. Jahnke, F. *et al.* Excitonic nonlinearities of semiconductor microcavities in the nonperturbative regime. *Phys. Rev. Lett.* **77,** 5257–5260 (1996).
80. Haroche, S. in *New Trends in Atomic Physics* (eds Grynberg, G. & Stora, R.) 193–309 (Elsevier, Oxford, 1984).
81. Kaluzny, Y., Goy, P., Gross, M., Raimond, J. M. & Haroche, S. Observation of self-induced Rabi oscillations in two-level atoms excited inside a resonant cavity: The ringing regime of superradiance. *Phys. Rev. Lett.* **51,** 1175–1178 (1983).
82. Carmichael, H. J., Tian, L., Ren, W. & Alsing, P. in *Cavity Quantum Electrodynamics* (ed. Berman, P. R.) 381–423 (Academic, Boston, 1994).

83. Kimble, H. J. in *Cavity Quantum Electrodynamics* (ed. Berman, P. R.) 203–266 (Academic, San Diego, 1994).
84. Lee, E. S. *et al.* Saturation of normal-mode coupling in aluminum-oxide-aperture semiconductor nanocavities. *J. Appl. Phys.* **89,** 807–809 (2003).
85. Houdré, R. *et al.* Measurement of cavity-polariton dispersion curve from angle-resolved photoluminescence experiments. *Phys. Rev. Lett.* **73,** 2043–2046 (1994).
86. Kira, M., Jahnke, F. & Koch, S. W. Microscopic theory of excitonic signatures in semiconductor photoluminescence. *Phys. Rev. Lett.* **81,** 3263–3266 (1998).
87. Kira, M., Hoyer, W., Stroucken, T. & Koch, S. W. Exciton formation in semiconductors and the influence of a photonic environment. *Phys. Rev. Lett.* **87,** 176401 (2001).
88. Hoyer, W., Kira, M. & Koch, S. W. Influence of Coulomb and phonon interaction on the exciton formation dynamics in semiconductor heterostructures. *Phys. Rev. B* **67,** 155113 (2003).
89. Chatterjee, S. *et al.* Excitonic photoluminescence in semiconductor quantum wells: Plasma versus excitons. *Phys. Rev. Lett.* **92,** 067402 (2004).
90. Koch, S. W., Meier, T., Hoyer, W. & Kira, M. Theory of the optical properties of semiconductor nanostructures. *Physica E* **14,** 45–52 (2002).
91. Hoyer, W. *et al.* Many-body dynamics and exciton formation studied by time-resolved photoluminescence. *Phys. Rev. B* **72,** 075324 (2005).
92. Szczytko, J. *et al.* Determination of the exciton formation in quantum wells from time-resolved interband luminescence. *Phys. Rev. Lett.* **93,** 137401 (2004).
93. Kira, M. *et al.* Quantum theory of nonlinear semiconductor microcavity luminescence explaining "boser" experiments. *Phys. Rev. Lett.* **79,** 5170–5173 (1997).
94. Pau, S. *et al.* Observation of a laserlike transition in a microcavity exciton polariton system. *Phys. Rev. B* **54,** R1789–R1792 (1996).
95. Cao, H. *et al.* Transition from a microcavity exciton polariton to a photon laser. *Phys. Rev. A* **55,** 4632–4635 (1997).
96. Mosor, S. *et al.* Scanning a photonic crystal slab nanocavity by condensation of xenon. *Appl. Phys. Lett.* **87,** 141105 (2005).
97. Badolato, A. *et al.* Deterministic coupling of single quantum dots to single nanocavity modes. *Science* **308,** 1158–1161 (2005).
98. Borri, P., Langbein, W., Woggon, U., Jensen, J. R. & Hvam, J. M. Microcavity polariton linewidths in the weak-disorder regime. *Phys. Rev. B* **63,** 035307 (2000).
99. Soljacic, M. & Joannopoulos, J. D. Enhancement of nonlinear effects using photonic crystals. *Nature Mater.* **3,** 211–219 (2004).
100. McCall, S. L. & Gibbs, H. M. in *Optical Bistability* (eds Bowden, C. M., Ciftan, M. & Robl, H. R.) 1–7 (Plenum, New York, 1981).
101. Sanchez-Mondragon, J. J., Narozhny, N. B. & Eberly, J. H. Theory of spontaneous-emission line shape in an ideal cavity. *Phys. Rev. Lett.* **51,** 550–553 (1983).
102. Brune, M. *et al.* Quantum Rabi oscillation: A direct test of field quantization in a cavity. *Phys. Rev. Lett.* **76,** 1800–1803 (1996).
103. Carmichael, H. & Orozco, L. A. Single atom lases orderly light. *Nature* **425,** 246–247 (2003).
104. Santori, C., Fattal, D., Vukovic, J., Solomon, G. S. & Yamamoto, Y. Indistinguishable photons from a single-photon device. *Nature* **419,** 594–597 (2002).
105. Imamoglu, A. *et al.* Quantum information processing using quantum dot spins and cavity QED. *Phys. Rev. Lett.* **83,** 4204–4207 (1999).
106. McKeever, J. *et al.* Deterministic generation of single photons from one atom trapped in a cavity. *Science* **303,** 1992–1994 (2004).
107. Cui, G. & Raymer, M. G. Quantum efficiency of single-photon sources in the cavity-QED strong-coupling regime. *Opt. Express* **13,** 9660–9665 (2005).
108. Cirac, J. I., Zoller, P., Kimble, H. J. & Mabuchi, H. Quantum state transfer and entanglement distribution among distant nodes in a quantum network. *Phys. Rev. Lett.* **78,** 3221–3224 (1997).
109. Keller, M., Lange, B., Hayasaka, K., Lange, W. & Walther, H. Deterministic coupling of single ions to an optical cavity. *Appl. Phys. B* **76,** 125–128 (2003).


## Acknowledgements

For financial support in Tucson: DARPA, NSF (AMOP and EPDT), AFOSR, and AFOSR DURINT; in Marburg: partially by the Deutsche Forschungsgemeinschaft through the Quantum Optics in Semiconductors Research Group and the Optodynamics Center of the Philipps-Universität Marburg; at Caltech: MURI Center for Photonic Quantum Information Systems (ARO/ARDA), NSF-ECS-NIRT and AFOSR.

## Competing financial interests

The authors declare that they have no competing financial interests.